Efficient Antenna Systems: Calibration of the Mars Deep Space Station 64-m Antenna System Noise Temperature Degradation Due to Quadripod Scatter

P. D. Potter

Communications Elements Research Section

In January 1973 extensive tests were performed of Mars Deep Space Station system noise temperature as a function of antenna elevation angle. These tests were performed under the ideal conditions of cold, dry weather, for which atmospheric absorption is well known. These data have been completely reduced and show a remarkably low residual to an elevation angle curve fit (less than 0.1 K). A new computer program has been developed which yields ground noise contribution as a function of antenna pointing direction and (known) direct feed system spillover. By subtracting the atmospheric and direct spillover effects out of the measured system temperature data, the noise temperature contribution of the quadripod scattering has been established to an accuracy of a few tenths of a kelvin. At low to moderate elevation angles, the effect is roughly twice as severe as at zenith. In this reporting, the data reduction procedure, computer program formulation and the results are presented.

I. Experimental Data

The extensive January 1973 tests performed on the DSS 14 reflex feed system have been previously described (Ref. 1). All four combinations of S- and X-band and reflex and non-reflex (standard) configurations were tested. As described in Ref. 1, the low-elevation angle noise temperature performance of the S-band reflex feed is superior to that of the standard S-Band Megawatt Transmit (SMT) (feed cone) performance. As will be described later in this article, the difference is predictable from the tricone geometry and the lower forward spillover of the S-band reflex systems. The observed effect has stimulated interest in the detailed noise temperature performance of the various feed systems.

The antenna gain was extensively tested, using radio source techniques. These gain tests were performed as a function of elevation angle by tracking a selected radio source (3C123) for a period of several hours, taking both on-source and off-source system temperature measurements. The off-source tests involved offsetting the

antenna pointing direction relative to source ephemeris position by a standard amount, typically 1 deg in azimuth. The noise adding radiometer (NAR)-determined system temperature and the station time were simultaneously printed on a digital recorder. From a knowledge of the source position and the time (printed to the closest second), the antenna elevation angle was accurately determined for the exact time the system off-source noise temperature was recorded, all without human error.

The measured temperature vs. elevation angle data so obtained was curve-fitted utilizing a JPL Scientific Computer Facility (SCF) cubic spline fitting program (Ref. 2). In reducing the data, the minimum number of spline breakpoints was used, compatible with a stable mean-square residual. Four days of data were available, 1/27/73 through 1/30/73, Universal Time. Each day's data (a single run) were separately curve fitted. The number of points per run varied from 26 to 72.

The largest data volume was for the S-band reflex configuration, with a total of 103 points (3 days of data) after combining the runs, with elevations from 8 to 85 deg. The RMS (i.e., 1 sigma) residual to the curve fit was 0.072 K. Spline breakpoints were used at 12, 22, 45, and 70 deg. The standard configuration (SMT feed cone) data consisted of 38 points (2 days), with elevations from 14 to 82 deg. Breakpoints were used at 45 and 70 deg, and an RMS (1 sigma) residual of 0.051 K relative to the curve fit was obtained.

The standard non-reflex X-band data were limited, unfortunately, to one run (1/30/73) of 17 points ranging from 50 to 84 deg elevation. No breakpoints were used and an RMS (1 sigma) residual of 0.012 K was obtained.

Interpretation of the X-band reflex data posed a special problem. Three runs were available: 1/28/73, 1/29/73, and 1/30/73. These data, when separately fitted, showed RMS residuals of 0.060, 0.050, and 0.093 K, respectively. However, the curve fits showed mean differences (for fixed elevation angles) between days of 0.5 to 1 K. If these large differences were ascribed to actual data noise, they would have to be interpreted as 10- to 20-sigma effects, which is statistically impossible. All tests were done by the same experimenters, offset from the same radio source and at the same times of day in each case. In all cases the weather was ideal: clear, dry, and cold. Thus it is virtually certain that either: (1) the receiving system changed between successive days, or (2) the NAR was not correctly adjusted in all cases. In no case is there evidence of a drift in the system temperature during a given run (several hours).

The above ambiguity cannot be resolved. After discussion with all of the parties involved, it was concluded that NAR misalignment was the most likely cause. The effect of such a misalignment is that all temperatures are incorrect by a fixed ratio close to unity. In combining the three X-band reflex data runs, therefore, two of them were multiplied by constant fixed ratios (2% and 5% different from unity) such that a minimum overall RMS of 0.080 K relative to the curve fit was obtained, a number comparable to the S-band data. The final X-band reflex data volume is 90 points, ranging from 8 to 85 deg elevation. The breakpoint values used were the same as for the S-band reflex data reductions.

Plots of the measured system temperature as a function of elevation angle were presented in Ref. 1 and are not repeated here. It is clear from these data that variations of several kelvins in antenna spillover effects occur as a function of elevation angle. The next section briefly describes a new computer program to analytically determine the effect of direct feed spillover upon noise temperature, as a function of feed design and antenna pointing direction.

II. Calculation of Direct Feed Spillover Noise Contribution

Figure 1 shows the ground noise contribution geometry. By a simple coordinate transformation it is found that the azimuthal angle, ϕ_E, corresponding to the horizon is given by

$$\cos \phi_E = \frac{\tan \alpha}{\tan \theta}, \qquad \theta \geq \alpha \qquad (1)$$

where

α = antenna elevation angle

θ = polar angle in the antenna coordinate system

The ground noise contribution, $T_{AG}(\alpha)$, is given in kelvins by (Ref. 3):

$$T_{AG}(\alpha) = \frac{\displaystyle\iint_{\text{GROUND}} T_{\text{GND}}(\alpha,\theta,\phi)\, P(\theta,\phi) \sin \theta \, d\phi \, d\theta}{\displaystyle\iint_{\substack{\text{ALL} \\ \text{SPACE}}} P(\theta,\phi) \sin \theta \, d\phi \, d\theta} \qquad (2)$$

where

$T_{\text{GND}}(\alpha,\theta,\phi)$ = ground brightness temperature, kelvins

$P(\theta,\phi)$ = relative power radiation pattern response of the antenna

It is seen from Eq. (2) that the antenna power pattern, $P(\theta, \phi)$, is merely a weighting function in the integration. Small errors in the pattern specification do not grossly affect the answer $T_{AG}(\alpha)$. Considering only direct feed spillover, and for DSN feed systems utilized to date, $P(\theta, \phi)$ is approximately independent of ϕ. Thus,

$$T_{AG}(\alpha) \approx \frac{\displaystyle\int_{\theta=\alpha}^{\theta=180°} P(\theta) \sin\theta \, d\theta \int_{\phi=0}^{\phi=\phi_E(\alpha,\theta)} T_{\text{GND}}(\alpha,\theta,\phi) \, d\phi}{\pi \displaystyle\int_{\theta=0}^{\theta=180°} P(\theta) \sin\theta \, d\theta} \tag{3}$$

where

$P(\theta)$ = the average power pattern

The brightness temperature of the ground, $T_{\text{GND}}(\alpha,\theta,\phi)$, is related to the ground physical temperature, T_{PHYS}, by

$$T_{\text{GND}}(\alpha,\theta,\phi) = T_{\text{PHYS}}\{1 - R^2[\psi(\alpha,\theta,\phi)]\} \tag{4}$$

where

$R[\psi(\alpha,\theta,\phi)]$ = magnitude of the ground voltage reflection coefficient

$\psi(\alpha,\theta,\phi)$ = ground grazing angle

If the antenna is circularly polarized,

$$T_{\text{GND}}_{\text{CP}}(\alpha,\theta,\phi) =$$
$$T_{\text{PHYS}} \left\{ 1 - \frac{R_V^2}{2}[\psi(\alpha,\theta,\phi)] - \frac{R_H^2}{2}[\psi(\alpha,\theta,\phi)] \right\} \tag{5}$$

where

$R_V[\psi(\alpha,\theta,\phi)]$ = ground reflection coefficient for vertical polarization

$R_H[\psi(\alpha,\theta,\phi)]$ = ground reflection coefficient for horizontal polarization

For dry desert terrain, values for $R_V[\psi(\alpha,\theta,\phi)]$ and $R_H[\psi(\alpha,\theta,\phi)]$ are given in Ref. 4. From geometry it can be determined that

$$\sin\psi(\alpha,\theta,\phi) = \cos\alpha \sin\theta \cos\phi - \sin\alpha \cos\theta \tag{6}$$

A simple computer program has been developed which evaluates Eq. (3) subject to Eqs. (5) and (6). The selected ground reflection coefficient is for DSS 14-type ground, based on the data in Ref. 4. The program input is the antenna radiation pattern, $P(\theta)$ (tabular data in JPL standard pattern format), and the ground physical temperature, T_{PHYS}. The next section describes computed results.

III. Results

For the DSN 64-m-diam antennas, calculation of direct forward spillover effects is slightly complicated by the tricone asymmetry. As shown in Fig. 2, the feedhorn axes are not parallel to the antenna axis. Consequently, for identical horn patterns and a given elevation angle, the forward ground spillover effect is more severe for the upper (SMT), Polarization Diversity S-Band (PDS) feed cone positions than it is for the lower X-Band Cassegrain Experimental (XCE) feed cone position. The direct rear spillover, which arises from the subreflector scatter characteristics, is approximately independent of tricone position for a given frequency and feedhorn pattern. Figures 3 through 6 show, among other things, the computed direct spillover noise contributions for the four possible systems, for a ground physical temperature of 15.5°C (60°F).

To determine the magnitude of the quadripod scatter effect, it was assumed that the system noise temperature was the sum of five components: (1) receiver/transmission line noise, (2) extra-atmospheric noise, (3) atmospheric noise loss, (4) direct spillover ground noise, and (5) quadripod scatter noise. At S-band, the atmospheric noise is not particularly dependent on humidity and has been very accurately determined as 2.2 kelvins (Ref. 5). At X-band, a zenith atmospheric noise contribution of 2.5 kelvins has been calculated by T. Otoshi of the Communications Elements Research Section for the clear, cold, dry conditions that prevailed for the January 1973 tests. The calculated atmospheric and direct spillover contributions were subtracted from the measured data described above, leaving a residual composed of items (1), (2) and (5). Items (1) and (2) are essentially elevation-angle independent; to determine their magnitude, it was assumed that the sum of items (4) and (5) have a value of 3.0 K at zenith. This value has been approximately determined experimentally (to within a few tenths of a kelvin) and was previously utilized in quadripod studies (Ref. 6). Using this information, the sum of (1) and (2) was determined, leaving only the quadripod component (5) as a residual. The resultant quadripod effect is shown

in Figs. 3 through 6 for the four systems. For the X-band reflex system, an additional component caused by dichroic plate reflection (Ref. 1) is present. The magnitude of this effect was determined (Fig. 6) by differencing out the quadripod effect determined for the nonreflex X-band operation.

Figure 7 shows the total ground noise contribution including direct spillover, quadripod scatter, and (for X-band reflex operation) dichroic plate scattering.

IV. Conclusion

By a combination of experimental data and computation, the DSS 14 quadripod-induced system noise temperature degradation has been determined as a function of antenna elevation angle. The magnitude is somewhat larger than that predicted for isotropic quadripod scattering (Ref. 6), but is in semiquantitative agreement. A possible technique for performance enhancement of the system by control of the quadripod scattering pattern has been previously suggested (Ref. 6).

References

1. Potter, P. D., "S- and X-Band Feed System," in *The Deep Space Network Progress Report*, Technical Report 32-1526, Vol. XV, pp. 54–62. Jet Propulsion Laboratory, Pasadena, Calif., June 15, 1973.

2. Hanson, R. J., "Computing Quadratic Programming Problems: Linear Inequality Constraints," Feb. 9, 1970 (JPL internal document).

3. Rusch, W. V. T., and Potter, P. D., *Analysis of Reflector Antennas*, pp. 71–73. Academic Press, New York, 1970.

4. Reed, H. R., and Russel, C. M., *Ultra High Frequency Propagation*, p. 97. John Wiley & Sons, New York, 1953.

5. Ho, W., et al., "Brightness Temperature of the Terrestrial Sky at 2.66 GHz," *J. Atmos. Sci.*, Vol. 29, pp. 1210–1212, September 1972.

6. Potter, P. D., "Antenna Study: Performance Enhancement," in *The Deep Space Network Progress Report*, Technical Report 32-1526, Vol. X, pp. 129–134. Jet Propulsion Laboratory, Aug. 15, 1972.
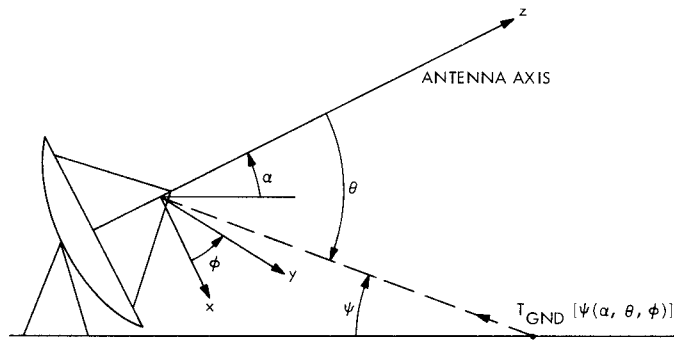
Fig. 1. Ground noise geometry
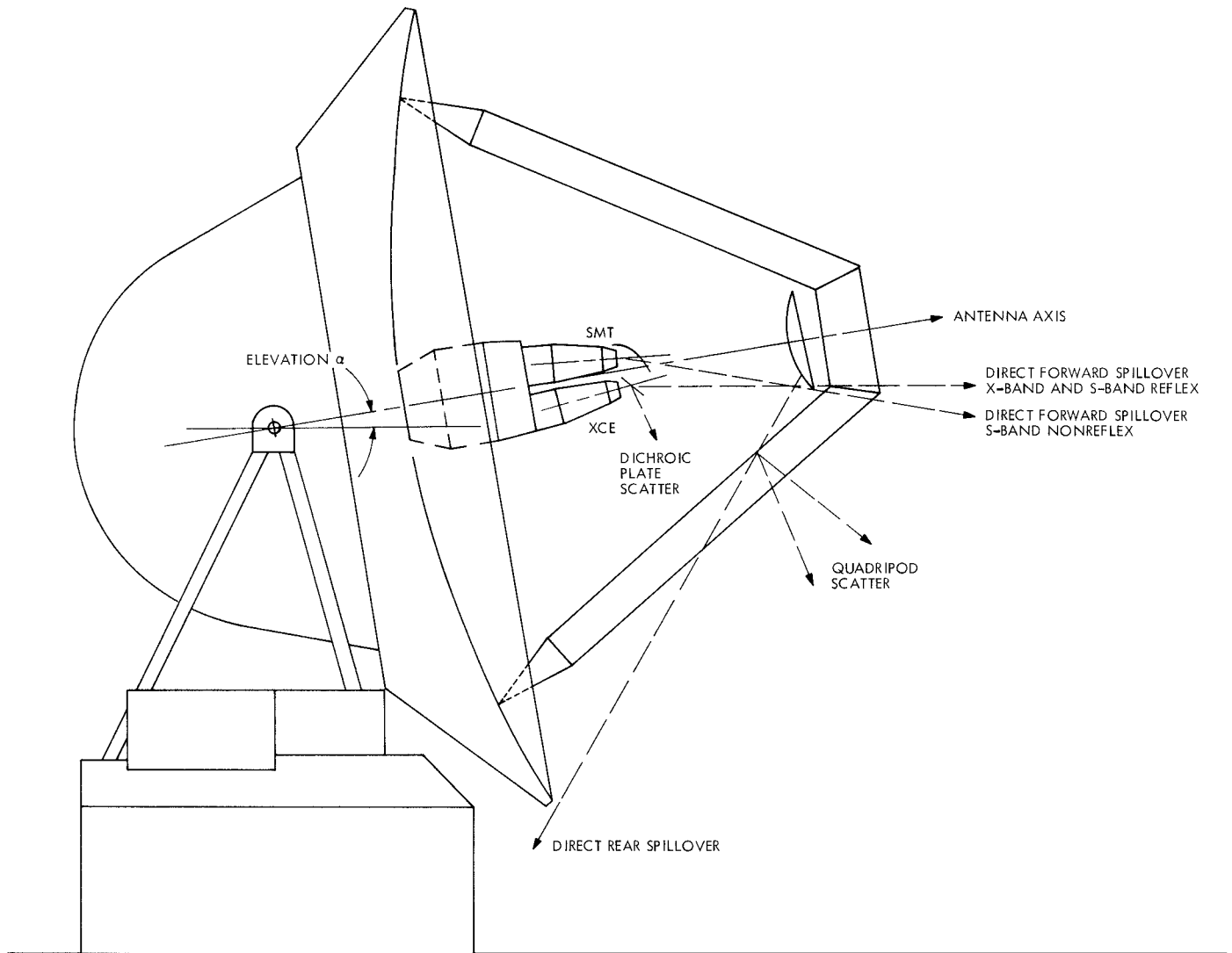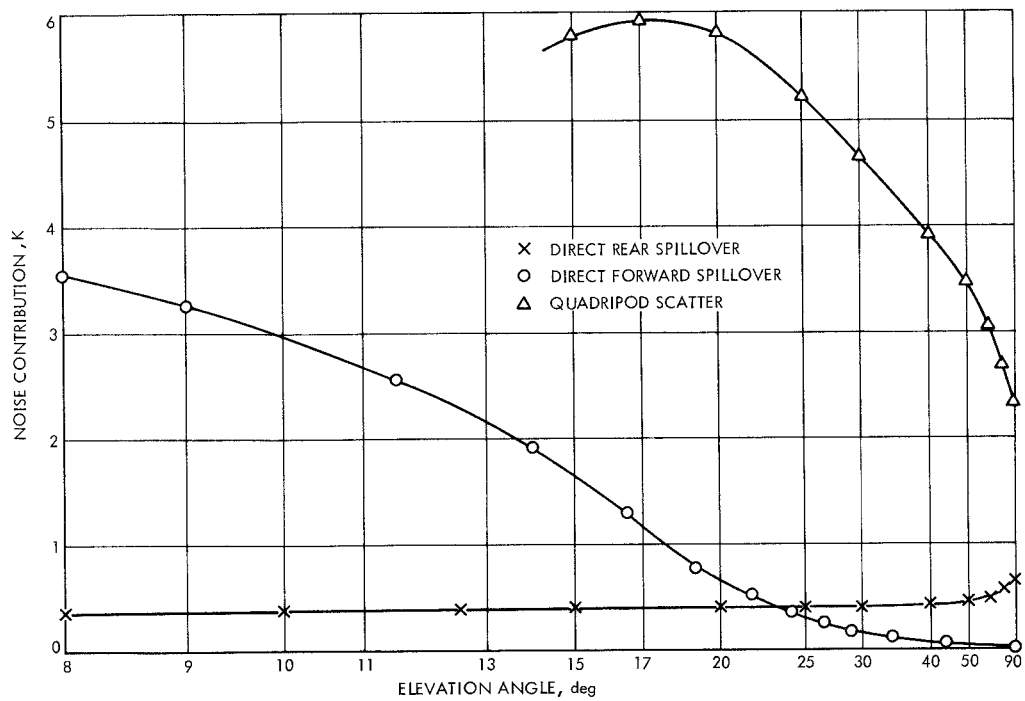

Fig. 2. DSS 14 spillover geometry

Fig. 3. DDS 14 dry ground noise contributions, S-band non-reflex (SMT)
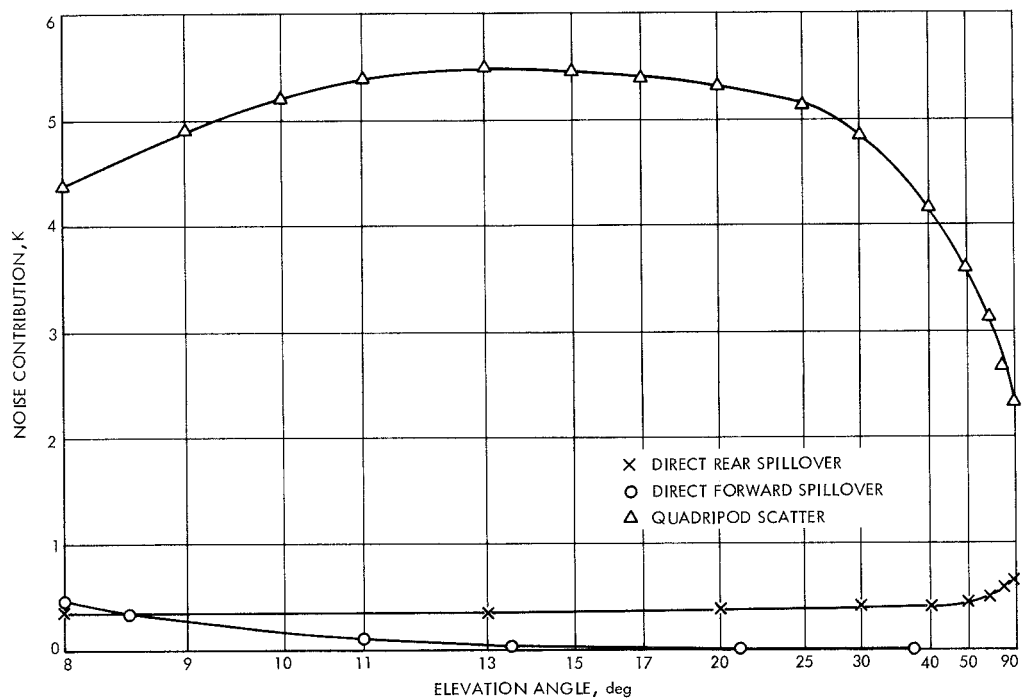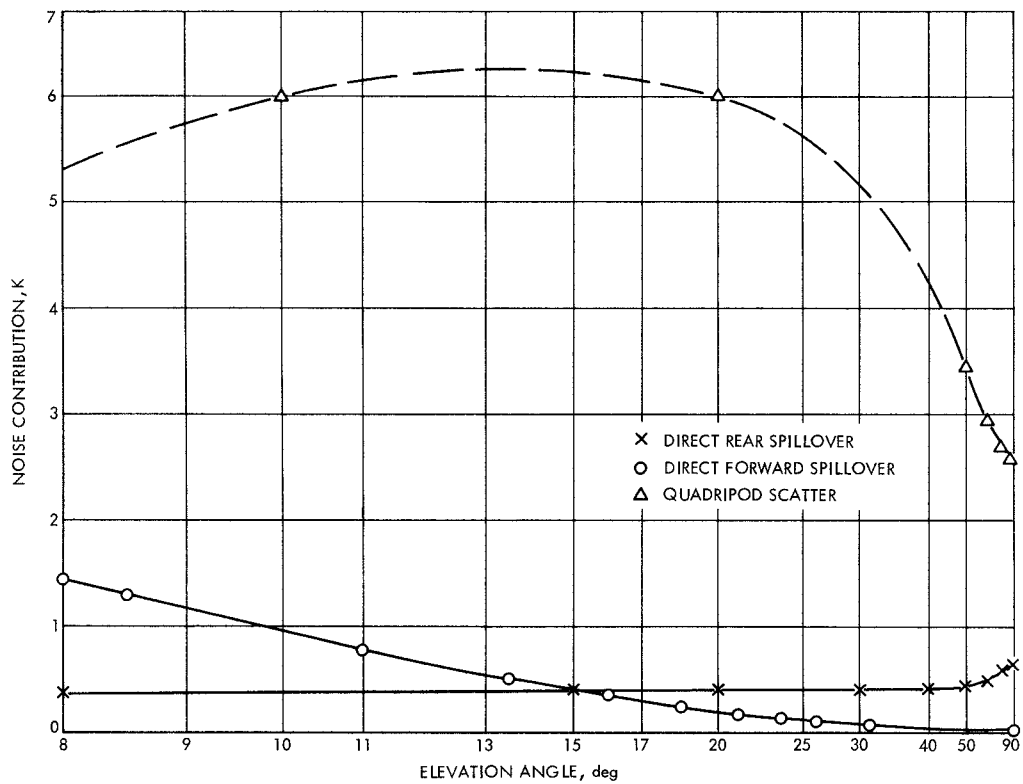

Fig. 4. DSS 14 dry ground noise contributions, S-band reflex

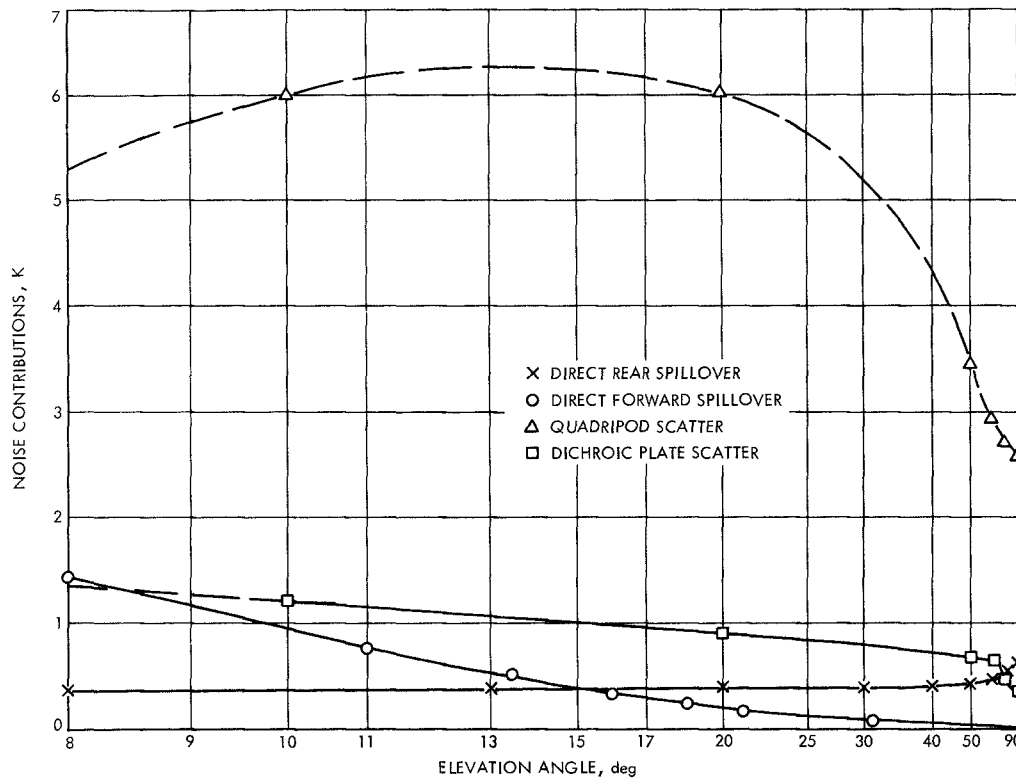Fig. 5. DSS 14 dry ground noise contributions, X-band non-reflex, X-band Cassegrain Experimental (XCE))
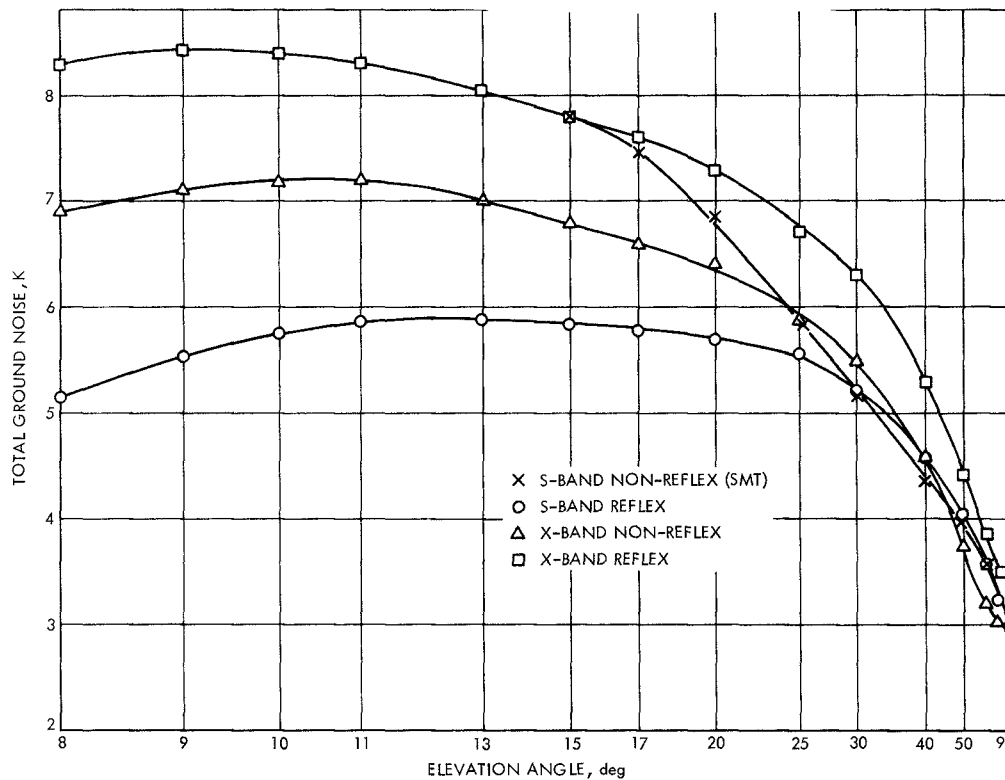
Fig. 6. DSS 14 dry ground noise contributions, X-band reflex

Fig. 7. DSS 14 dry ground total ground noise